J Solid State Electrochem (2012) 16:2329–2333
DOI 10.1007/s10008-012-1731-6

ORIGINAL PAPER

Switching transition states with changing electrode potential: Zn(II)/Zn electrodeposition on glassy carbon in the *N*-butyl-*N*-methylpyrrolidinium bis(trifluoromethylsulfonyl)imide ionic liquid

Sven Ernst · Martin C. Henstridge · Richard G. Compton

Received: 3 February 2012 / Revised: 29 February 2012 / Accepted: 4 March 2012 / Published online: 31 March 2012

Abstract The mechanisms for the electrodeposition and stripping of $Zn^{2+}|Zn$ in the *N*-butyl-*N*-methylpyrrolidinium bis(trifluoromethylsulfonyl)imide ionic liquid are investigated via cyclic voltammetry. Analysis showed that the deposition of Zn onto a bulk Zn surface occurred via a two-electron process, with the first electron transfer being rate determining. The electrodissolution was found to occur via a potential-dependent mechanism with the first electron transfer being rate determining near the formal potential, while an intermediate chemical step became rate determining at more positive potentials.

Keywords Zinc · Electrodeposition · Electrodissolution · Ionic liquid · Multi-electron process · Voltammetry

Introduction

In a multi-electron process, the rate-determining step can change with potential, although examples of this effect are rare. Below, the example of the two-electron reduction of zinc(II), in the ionic liquid *N*-butyl-*N*-methylpyrrolidinium bis(trifluoromethylsulfonyl)imide $[C_4mPyrr][NTf_2]$, is used to demonstrate a change in the mechanism of anodic Zn dissolution.

Applying the principle of microscopic reversibility to electron transfer reactions suggests that oxidation and reduction should both occur via the same pathway. Consequently, for the generalised multi-electron process,

$$A \pm ne^- \rightleftarrows B \tag{1}$$

both the forward and back reactions should proceed via the same transition state. As such the cathodic (α) and anodic (β) Butler–Volmer electron transfer coefficients, which indicate the position of the transition state, are related via $\alpha + \beta = n$, where n represents the total number of electrons transferred. This relationship holds for a given potential, but during a voltammetric experiment the potential is varied, causing changes in the local energetic environment such as altering the electrode solvation and/or double-layer properties. As such the relative position of the transition state may vary as the potential changes, resulting in potential-dependent transfer coefficients.

The transfer coefficient can only be measured when faradaic current is passed; it is therefore only possible to measure α at reducing potentials and β at oxidising potentials. Thus for irreversible electrochemical systems, which exhibit highly separated reductive and oxidative peaks, the potentials at which the two transfer coefficients are measured may differ greatly. As such it is possible to measure $\alpha + \beta \neq n$ without violating the principle of microscopic reversibility [1–3]. The switch of β with potential for the oxidation of Zn is reported below.

The electrodeposition and anodic dissolution of zinc has been studied previously in aqueous, [4–10] molecular organic [11–13] and ionic liquid [14–22] systems, largely in the field of corrosion research. However, there is debate as to the mechanisms of zinc electrodeposition and dissolution in the various solvents. Cachet and Wiart have studied the anodic dissolution of zinc in aqueous chloride [4] and sulphate [5, 6] solutions, proposing complex mechanisms involving up to

This study is to be submitted to the *Journal of Solid State Electrochemistry*.

S. Ernst · M. C. Henstridge · R. G. Compton (✉)
Department of Chemistry, Physical and Theoretical Chemistry Laboratory, Oxford University,
South Parks Road,
Oxford OX1 3QZ, UK
e-mail: richard.compton@chem.ox.ac.uk

three parallel dissolution paths and up to three adsorbed intermediates: Zn^{+}_{ads}, Zn^{2+}_{ads} and $Zn(OH)^{+}_{ads}$.

Banaś et al. studied Zn stripping, from a zinc anode, in methanolic and aqueous lithium chloride solutions, both in the presence and in the absence of oxygen [11]. In the deoxygenated methanolic system, the anodic dissolution of zinc was found to occur via two separate mechanisms, depending on overpotential. The Tafel analysis performed by Banaś et al. yielded slopes of ~40 and ~120 mV/decade, depending on the overpotential. These values correspond to a transfer coefficient of ~1.5 near the formal potential, changing to ~0.5 at higher overpotential. Furthermore, Banaś et al. found that the anodic dissolution of Zn was hindered by the formation of a passivating layer when the methanolic solutions were exposed to oxygen or when the experiment was carried out in de/oxygenated H_2O.

More recent work by Światowska-Mrowiecka and Banaś investigated the anodic stripping of zinc from distinct (0001) and $(11\bar{2}0)$ crystal faces in deoxygenated, methanolic, lithium perchlorate solutions [12]. This work found that the anodic dissolution of zinc proceeds via a two-step mechanism with a fast, quasi-reversible formation of Zn^{+}_{ads} followed by the rate-determining step yielding Zn^{2+}. Furthermore, in contrast to the earlier work by Banaś et al., the two redox waves were shown to be separated by circa 300 mV [12].

Pérez et al. found that the reduction of Zn^{2+} to Zn(Hg) in 1 M aqueous $NaClO_4$ proceeds via an EEC mechanism, with electron transfer coefficients of 0.45, 0.52 and 0.982 for the respective steps [7]. Hassan et al. demonstrated that a surface ZnO and $Zn(OH)_2$/ZnO passivating film was formed during anodic dissolution in aqueous perchlorate solutions, with the passivating nature of the film decreasing upon deoxygenation of the solutions [8–10].

Białozór and Bandura studied the electrodeposition and stripping of Zn from dimethyl sulphoxide (DMSO), *N*,*N*-dimethylformamide (DMF) and acetonitrile (ACN), finding that in all cases the reaction involved two one-electron transfers [13]. Furthermore, while the cathodic transfer coefficient, α, was found to be ~0.5 in all three solvents, the anodic transfer coefficient, β, was found to be ~0.5 in DMSO and ~1 in DMF and ACN [13]. This work by Białozór and Bandura represents, to the best of the authors' knowledge, the only insights into the electron transfer mechanisms of Zn electrodeposition and stripping from aprotic solvents and suggests that in all of the solvents studied the electrodeposition and stripping of Zn proceeds via the two-step mechanism [13]:

$$Zn^{2+} + e^{-} \rightleftarrows Zn^{+} \tag{2.1}$$

$$Zn^{+} + e^{-} \rightleftarrows Zn \tag{2.2}$$

where the Zn^{+} intermediate and possibly the Zn^{2+} intermediate may be adsorbed on the electrode surface. Although this is not mentioned directly in the paper by Białozór and Bandura [13], analogy to the protic systems mentioned above suggests that this is a reasonable assumption. Furthermore, Białozór and Bandura also observed that in ACN, multicyclic voltammograms gave decreased reduction peaks, as a passivating layer was formed via a secondary chemical reaction, whereby it was speculated that anion radicals were formed via:

$$Zn^{+} + R \rightleftarrows Zn^{2+} + R^{-} \tag{2.3}$$

and the R^{-} radicals then initiated the polymerisation of solvent molecules and the adsorption of these products on the cathodic scan caused a partial blocking of the electrode surface [13]. However, Białozór and Bandura did not rule out the possibility that the anion radicals were formed via the electrocatalytic reduction of solvent molecules on the freshly deposited zinc.

The electrodeposition of Zn has also been studied in room temperature ionic liquids (RTILs), with papers describing deposition from chlorozincate [14] and chloroaluminate [15] imidazolium molten salts, choline chloride-based deep eutectic solvents [16–19], tributylmethylammonium bis(trifluoromethylsulfonyl)imide [20] and *N*-butyl-*N*-methylpyrrolidinium dicyanamide [21, 22]. However, these papers focus on the morphologies of Zn deposits, as well as crystal nucleation/growth mechanisms, as opposed to the electron transfer mechanisms involved and are primarily concerned with the electroplating of zinc.

The present work investigates the electron transfer mechanisms for the Zn^{2+}|Zn electrodeposition and stripping in a $[C_4mPyrr][NTf_2]$ ionic liquid by cyclic voltammetry. The $[C_4mPyrr][NTf_2]$ ionic liquid was chosen for its large potential window as well as its persistence under vacuum, which reduces the probability of forming the passivating oxide/hydroxide layers seen previously in aqueous and non-aqueous systems [4–6, 8–13]. Furthermore, zinc was introduced to the ionic liquid as a bis(trifluoromethylsulfonyl)imide salt, $Zn[NTf_2]_2$, so as to minimise confusion around Zn(II) speciation [21, 22] and the effects of anions on zinc electrodissolution, seen previously in aqueous [23] and organic [11] systems.

Experimental

$[C_4mPyrr][NTf_2]$ (electrochemically pure) was kindly donated by Queens University, Belfast. Zinc oxide (ZnO, 99 %) was obtained from Sigma Aldrich. Bis(trifluoromethane)sulfonimide ($H[NTf_2]$, >95 %) was obtained from Fluka. Silver trifluoromethanesulfonate (>99.95 %) was obtained from Aldrich. ACN (HPLC grade) was obtained from Fischer scientific. $Zn[NTf_2]_2$ was synthesised by adding 50 % molar excess ZnO to an aqueous solution of

H[NTf_2] and stirring overnight before filtering through a sintered glass frit and drying under rotary evaporation followed by high vacuum overnight.

Electrochemical measurements were performed in a thermostated (25.0±0.1 °C) Faraday cage, using a μAutolab Type II computer-controlled potentiostat (Ecochemie). All measurements were obtained using a standard three-electrode configuration, employing a glassy carbon (GC, r=1.5 mm, BASi) working electrode, a platinum mesh (99.9 %, Goodfellow) counter electrode and a Ag/Ag^+ reference electrode (see below). Prior to use the working electrode was polished using 1, 0.3 and 0.05 alumina lapping compounds (Buehler) on soft lapping pads (Buehler) before being placed in deionised water (resistivity >18.2 MΩ cm at 25 °C, Millipore water systems) in an ultrasonic bath for ~3 min to remove any adsorbed material. The working electrode was then rinsed thoroughly with ACN and dried using compressed air. Before use, the counter electrode was cleaned in a hot Bunsen flame before being rinsed thoroughly with ACN. The Ag/Ag^+ reference electrode was prepared following the method of Meng et al. [24] and yielded a reproducible formal potential for the ferrocene|ferrocenium couple of -379±3 mV at the GC electrode in [C_4mPyrr][NTf_2].

The experiment was prepared by placing 100 μl of 100 mM Zn[NTf_2]$_2$ in [C_4mPyrr][NTf_2] into a sample chamber on top of the GC electrode, constructed by placing a section of micropipette tip (Eppendorf) over the electrode tip. The working electrode and sample were then placed into a glass T-shaped cell, described previously [25], and the counter and reference electrodes fed into the sample from above. One arm of the T-shaped cell was then connected to a rotary vacuum pump, and the sample was placed under vacuum for 2 h before measurement and remained under vacuum for the duration of the experiment. Studying the system in vacuo brings the water content of the RTIL to an acceptably low level [26].

Results and discussion

A 100 mM solution of Zn[NTf_2]$_2$ in [C_4mPyrr][NTf_2] was placed under vacuum to remove any residual H_2O and O_2 present, as these species have previously been shown to interfere with electrochemical measurements in ionic liquids [26–29]. Cyclic voltammograms (CVs) were then recorded for the electrodeposition and stripping of Zn on the GC working electrode. One such CV is shown in Fig. 1, where the potential was scanned from 0 to −1.8 and back to 0 V (vs. Ag/Ag^+) at a rate of 10 mV/s and a step size of ~1 mV. Evident in the figure are two peaks, $E_{p,c}$ and $E_{p,a}$, representing the cathodic and anodic processes, respectively. Also evident is the so-called nucleation loop, where the currents of the forward and reverse sweeps cross over. This nucleation loop is characteristic of systems in which metals are deposited onto foreign substrates, as a higher overpotential is required for nucleation at the surface than for the growth of an existing deposit [30]. The cathodic and anodic peaks $E_{p,c}$ and $E_{p,a}$ occur at −1.44 and −0.85 V vs. Ag/Ag^+, respectively.

The mechanisms behind electrochemical processes can often be elucidated with the help of Tafel analysis where, for a multiple electron mechanism, a plot of ln(I) vs. E allows the rate-limiting step to be determined, for a reduction [31, 32], via:

$$\frac{\partial \ln(I)}{\partial E} = \frac{-(n' + \alpha_{n'}) \cdot F}{R \cdot T} \tag{3.1}$$

or for an oxidation [31, 32] via:

$$\frac{\partial \ln(I)}{\partial E} = \frac{(n' + \beta_{n'}) \cdot F}{R \cdot T} \tag{3.2}$$

where I is the current, E the potential, n' the number of electrons transferred before the rate-limiting step and $\alpha_{n'}$ and $\beta_{n'}$ are the electron transfer coefficients of the rate-determining steps for the reduction and oxidation, respectively. F is Faraday's constant, R the universal gas constant and T the temperature.

In order to analyse the mechanisms involved in the electrodeposition and stripping of the Zn^{2+}|Zn couple, omitting the nucleation and growth of Zn on the glassy carbon phase, a plot of ln(I) vs. E was constructed from the reverse scan shown in Fig. 1. This plot yielded three linear Tafel regions, which are highlighted above in Fig. 1 and presented as Figs. 2, 3 and 4.

Figures 2, 3 and 4 show Tafel plots of ln(I) vs. E for the deposition and stripping of the Zn^{2+}|Zn couple in [C_4mPyrr][NTf_2], constructed using data shown in Fig. 1. The figures highlight the three distinct Tafel regions shown as α, β_1 and β_2 in Fig. 1. The regression lines for α, β_1 and β_2 in Figs. 2, 3 and 4 were found to be $\ln(I)=-24.62E-44.93$, $\ln(I)=19.30E+8.738$ and $\ln(I)=45.83E+38.13$, respectively,

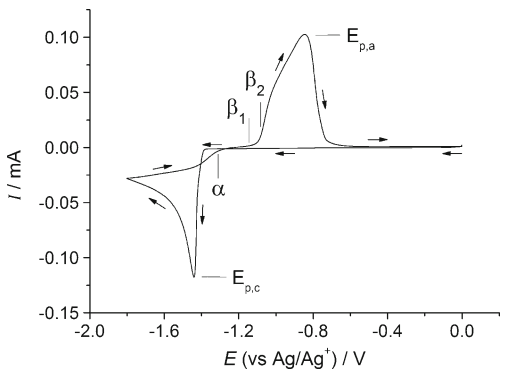

Fig. 1 CV showing the electrodeposition and stripping of Zn^{2+}|Zn onto a GC electrode in [C_4mPyrr][NTf_2], recorded at 25 °C and 10 mV/s. The symbols α, β_1 and β_2 indicate the regions on the curve which gave the Tafel plots described in the text

having adjusted R^2 values of 0.99981, 0.99998 and 0.99991, respectively. The values of ($n_1'+\alpha$), ($n_2'+\beta_1$) and ($n_3'+\beta_2$), obtained from the slopes of the lines of best fit in Figs. 2, 3 and 4 via (3), were found to be 0.63±0.09, 0.57±0.09 and 1.13±0.07, respectively (where the values and uncertainties were derived from averaged measurements). The value for the cathodic transfer coefficient (α) of 0.63±0.09 suggests that n_1' equals zero, and hence, the first electron transfer is rate determining. Thus the electrodeposition of Zn^{2+} onto Zn proceeds via:

$$Zn^{2+}_{(RTIL)} + e^- \overset{slow}{\rightarrow} Zn^{+}_{(ads/RTIL)} \tag{4.1}$$

$$Zn^{+}_{(ads/RTIL)} + e^- \overset{fast}{\rightleftarrows} Zn_{(s)} \tag{4.2}$$

where the subscripts (RTIL) and (s) refer to the solvated and solid states, respectively, while the subscript (ads/RTIL) refers to the fact that the Zn^+ species may be adsorbed, solvated or a combination of the two. To the best of the authors' knowledge, there have been no reports as to the nature of Zn^{2+} and Zn^+ solvation in the [C_4mPyrr][NTf_2] RTIL, however the possibility of ion pairing cannot be ruled out. The value of the anodic transfer coefficient close to the formal potential (β_1), 0.57±0.09, suggests that n_2' is zero and the first electron transfer is again rate limiting. Thus, the electrodissolution of Zn from the bulk zinc surface at potentials close to the formal potential occurs via:

$$Zn_{(s)} \overset{slow}{\rightarrow} Zn^{+}_{(ads/RTIL)} + e^- \tag{5.1}$$

$$Zn^{+}_{(ads/RTIL)} \overset{fast}{\rightleftarrows} Zn^{2+}_{(RTIL)} + e^- \tag{5.2}$$

However, as the potential is swept to increasingly positive values, a shift in the anodic transfer coefficient from 0.57±0.09 ($n_2'+\beta_1$) to 1.13±0.07 ($n_3'+\beta_2$) implies a change of mechanism, with $n_3'=1$, and the stripping occurs via an ECE mechanism where the first, now fast, step is given by:

$$Zn_{(s)} \overset{fast}{\rightleftarrows} Zn^{+}_{(ads/RTIL)} + e^- \tag{6.1}$$

This fast step is then followed by the rate-determining chemical step, which may be one of the following:

$$Zn^{+}_{(ads)} \overset{slow}{\rightarrow} Zn^{+}_{(RTIL)} \tag{6.2.1}$$

$$Zn^{+}_{(RTIL)}(A) \overset{slow}{\rightarrow} Zn^{+}_{RTIL}(B) \tag{6.2.2}$$

$$2Zn^{+}_{(ads/RTIL)} \overset{slow}{\rightarrow} Zn_{(s)} + Zn^{2+}_{(ads/RTIL)} \tag{6.2.3}$$

representing desorption, a change in solvation (where (A) and (B) represent different solvated states) or disproportionation, respectively. This slow, rate-determining chemical step is then followed by another fast electrochemical step:

$$Zn^{+}_{(ads/RTIL)} \overset{fast}{\rightleftarrows} Zn^{2+}_{(RTIL)} + e^- \tag{6.3}$$

Thus the rate-determining step of the electrodissolution of Zn switches as the potential is swept further in the positive direction. Note that the stripping of Zn occurs from

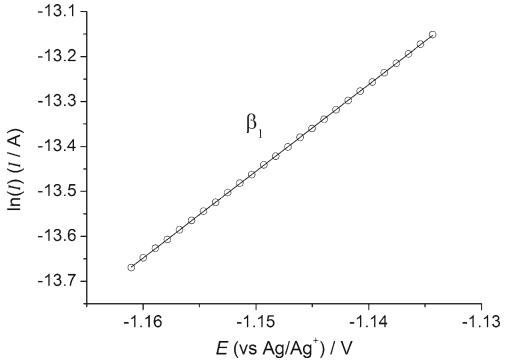

Fig. 3 Tafel plot for the stripping of Zn from Zn close to the formal potential of the Zn^{2+}|Zn couple

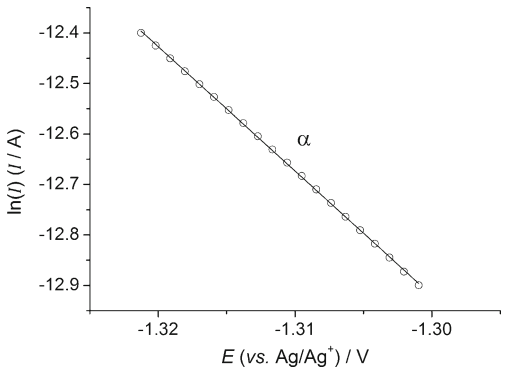

Fig. 2 Tafel plot for the deposition of Zn onto Zn close to the formal potential of the Zn^{2+}|Zn couple

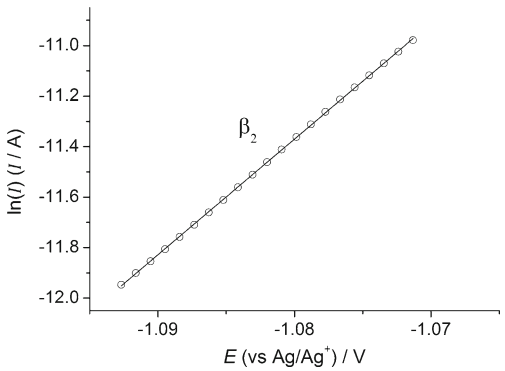

Fig. 4 Tafel plot for the stripping of Zn from Zn further from the formal potential of the Zn^{2+}|Zn couple

the bulk Zn surface, not from the GC electrode, at the potentials of β_1 and β_2 as even at $E_{p,a}$ approximately 24 layers of Zn remain on the electrode (based on $m/A=Q/nFA$ comparisons to an ideal monolayer of basal plane Zn).

It has been demonstrated in this work that the electrodeposition of zinc occurs via an EE or ECE mechanism, with the first reduction step being rate limiting. Furthermore, the electrodissolution of the deposited layer occurs either through an EE or ECE mechanism, with the first E step being rate limiting at potentials near the formal potential and a chemical step becoming rate limiting at more positive potentials.

Conclusion

The electrodeposition and stripping of the $Zn^{2+}|Zn$ couple onto and from a bulk zinc deposit on a glassy carbon electrode has been investigated in the $[C_4mPyrr][NTf_2]$ ionic liquid. The cathodic and anodic Tafel behaviour was analysed, and a single cathodic and two anodic electron transfer coefficients were found to be 0.63±0.09, 0.57±0.09 and 1.13±0.07, respectively. This implies that the electrodeposition of Zn occurs via an EE or ECE mechanism with the first step being rate determining, while the electrodissolution of Zn occurs via two different mechanisms depending on the applied potential. Close to the formal potential, the stripping occurs via an EE or ECE mechanism with a rate-determining first step; however, at more positive potentials, a chemical step occurring after the initial electron transfer becomes rate limiting and hence the mechanism shifts to an ECE form.

Acknowledgments The authors thank Dr. Sarah Norman and Prof. Chris Hardacre from Queen's University Ionic Liquid Laboratories for kindly donating the ionic liquid. SE thanks St. John's College Oxford and Syngenta for partial funding. MCH thanks EPSRC for the funding (EP/H002413/1).

References

1. Savéant J-M, Tessier D (1982) Faraday Discuss Chem Soc 74:57–72
2. Corrigan DA, Evans DH (1980) J Electroanal Chem 106(C):287–304
3. Suwatchara D, Henstridge MC, Rees NV, Compton RG (2011) J Phys Chem C 115(30):14876–14882
4. Cachet C, Wiart R (1981) J Electroanal Chem Interfacial Electrochem 129(1–2):103–114
5. Cachet C, Ganne F, Maurin G, Petitjean J, Vivier V, Wiart R (2001) Electrochim Acta 47(3):509–518
6. Cachet C, Ganne F, Joiret S, Maurin G, Petitjean J, Vivier V, Wiart R (2002) Electrochim Acta 47(21):3409–3422
7. Pérez M, Baars A, Zevenhuizen SJM, Sluyters-Rehbach M, Sluyters JH (1995) J Electroanal Chem 397(1–2):87–92
8. Hassan HH (2001) Appl Surf Sci 174(3–4):201–209
9. Hassan HH (2006) Electrochim Acta 51(26):5966–5972
10. Hassan HH, Amin MA, Gubbala S, Sunkara MK (2007) Electrochim Acta 52(24):6929–6937
11. Banaś J, Schütze KG, Heitz E (1986) J Electrochem Soc 133 (2):253–259
12. Światowska-Mrowiecka J, Banaś J (2005) Electrochim Acta 50 (9):1829–1840
13. Białłozór S, Bandura ET (1987) Electrochim Acta 32(6):891–894
14. Lin Y-F, Sun IW (1999) Electrochim Acta 44(16):2771–2777
15. Dogel J, Freyland W (2003) Phys Chem Chem Phys 5(12):2484–2487
16. Abbott AP, Barron JC, Ryder KS (2009) Trans Inst Met Finish 87 (4):201–207
17. Whitehead AH, Polzler M, Gollas B (2010) J Electrochem Soc 157 (6):D328–D334
18. Abbott AP, Barron JC, Frisch G, Gurman S, Ryder KS, Fernando Silva A (2011) Phys Chem Chem Phys 13 (21):10224–10231
19. Abbott AP, Barron JC, Frisch G, Ryder KS, Fernando Silva A (2011) Electrochim Acta 56(14):5272–5279
20. Chen P-Y, Hussey CL (2007) Electrochim Acta 52(5):1857–1864
21. Deng M-J, Chen P-Y, Leong T-I, Sun IW, Chang J-K, Tsai W-T (2008) Electrochem Commun 10(2):213–216
22. Deng M-J, Lin P-C, Chang J-K, Chen J-M, Lu K-T (2011) Electrochim Acta 56(17):6071–6077
23. Yu J, Yang H, Ai X, Chen Y (2002) Russ J Electrochem 38 (3):321–325
24. Meng Y, Aldous L, Belding SR, Compton RG (2012) Phys Chem Chem Phys. doi:10.1039/C2CP23801B
25. Evans RG, Klymenko OV, Price PD, Davies SG, Hardacre C, Compton RG (2005) ChemPhysChem 6(3):526–533
26. O'Mahony AM, Silvester DS, Aldous L, Hardacre C, Compton RG (2008) J Chem Eng Data 53(12):2884–2891
27. Buzzeo MC, Klymenko OV, Wadhawan JD, Hardacre C, Seddon KR, Compton RG (2003) J Phys Chem A 107(42):8872–8878
28. Huang XJ, Rogers EI, Hardacre C, Compton RG (2009) J Phys Chem B 113(26):8953–8959
29. Zhao C, Bond AM, Compton RG, O'Mahony AM, Rogers EI (2010) Anal Chem 82(9):3856–3861
30. Endres F, MacFarlane DR, Abbott AP (eds) (2008) Electrodeposition from ionic liquids. Wiley-VCH, Weinheim
31. Bockris JOM, Reddy AKN (1998) Modern electrochemistry, vol 1. Plenum, New York
32. Compton RG, Banks CE (2011) Understanding voltammetry, 2nd edn. World Scientific, Singapore